IIETA International Information and Engineering Technology Association
Advancing the World of Information and Engineering

Annales de Chimie - Science des Matériaux
Vol. 50, No. 5, October, 2026, pp. 463-473
Journal homepage: http://iieta.org/journals/acsm

Chemical Resistance and Microstructural Evolution of Fiber-Reinforced Self-Compacting Concrete Exposed to Acid and Sulfate Solutions

Ammar Hamlaoui[1], Rachid Djebien[2*], Salah Messast[2], Sara Rais[3]

[1] Department of Civil Engineering, Faculty of Sciences and Technology, University Echahid Cheikh Larbi, Tebessi 12002, Algeria
[2] Department of Civil Engineering, Faculty of Technology, 20 August 1955 University of Skikda, Skikda 21000, Algeria
[3] Department of Civil Engineering and Hydraulic, University Mohamed Khider, Biskra 07000, Algeria

Corresponding Author Email: r.djebien@univ-skikda.dz

Copyright: ©2026The authors. This article is published by IIETA and is licensed under the CC BY 4.0 license (http://creativecommons.org/licenses/by/4.0/).

https://doi.org/10.18280/acsm.500505

Received: 19 June 2026
Revised: 2 August 2026
Accepted: 17 August 2026
Available online: 31 October 2026

Keywords:
self-compacting concrete, waste polyethylene terephthalate fibers, compressive strength loss, scanning electron microscopy analysis, valorization

ABSTRACT

This study investigates the chemical resistance of self-compacting concrete (SCC) reinforced with conventional steel fibers (CSF), tire-derived steel fibers (TDSF), and waste polyethylene terephthalate (PET) fibers (WPF) recovered from discarded plastic packaging straps. Fiber contents of 0.5%, 1.0%, 1.5%, and 2.0% by volume were considered. The specimens were exposed to 5% H_2SO_4, 5% HCl, and 5% Na_2SO_4 solutions for 90 and 180 days. Mass and compressive strength losses were quantified, while scanning electron microscopy (SEM) was employed to characterize the microstructural damage induced by chemical exposure. The results revealed that the degradation behavior was strongly influenced by the fiber type, fiber content, exposure duration, and chemical environment. Under HCl exposure, WPF exhibited the most favorable performance, reducing the compressive strength loss to 12.60% at a fiber content of 2%. Similarly, under Na_2SO_4 exposure, the incorporation of 2% WPF limited the compressive strength loss to 1.70%. In contrast, under H_2SO_4 exposure, TDSF proved to be the most effective reinforcement, resulting in the lowest compressive strength loss of 6.96%. SEM observations revealed the formation of ettringite under sulfate attack, the dissolution of calcium silicate hydrate (C-S-H) gel and gypsum precipitation under acidic conditions, as well as the presence of fiber-matrix interfacial gaps around WPF.

1. INTRODUCTION

Self-compacting concrete (SCC) is regarded as one of the most significant achievements in modern concrete technology, distinguished by its exceptional rheological properties, including high flowability, the ability to fill formwork and pass through reinforcement bars without mechanical vibration, while maintaining internal homogeneity and high resistance to segregation [1, 2]. Major advances in chemical admixtures and cementitious materials have contributed to enhancing the rheological properties of SCC, thereby facilitating the incorporation of various types of fibers and recycled waste materials into its mix design [3, 4]. Nevertheless, despite its superior fresh-state properties, SCC remains susceptible to significant durability challenges in environments exposed to severe chemical attack such as sewage networks and industrial facilities, making the investigation of its behavior under acid and sulfate attack an important research need [5]. The long-term performance of construction materials is commonly assessed by comparing their properties before and after environmental exposure. For example, Ferrari et al. [6] investigated the characterization and aging-related durability of cool materials through standardized thermal performance evaluation.

On the other hand, the chemical durability of concrete represents one of the most complex areas of structural research. Aggressive environments involving mineral acids such as H_2SO_4, HCl, and sulfates Na_2SO_4 induce distinct deterioration mechanisms that target the primary hydration products, namely portlandite ($Ca(OH)_2$) and calcium silicate hydrate (C-S-H) gel. Sulfuric acid promotes the formation of gypsum and secondary ettringite, leading to the development of destructive expansive stresses, whereas hydrochloric acid produces highly soluble calcium chloride, thereby accelerating matrix decomposition and leaching [7]. These combined attacks result in progressive loss of mass and compressive strength, posing a long-term threat to structural integrity [8, 9].

The incorporation of conventional steel fibers (CSF) into SCC has been shown to effectively enhance crack resistance and energy absorption, thereby retarding the penetration of chemical attack into the interior of the matrix [10, 11]. However, the progressive corrosion of these fibers in acidic environments reduces their effectiveness and weakens the fiber-matrix interfacial transition zone (ITZ), highlighting the need to explore alternative fibers with greater chemical durability and environmental sustainability [12, 13].

In parallel, the world is facing a critical increase in solid waste volumes generated by rapid industrialization and

urbanization. The cement and concrete industry alone accounts for approximately 7–8% of total global CO_2 emissions, making the development of sustainable and environmentally friendly concrete an advanced research and engineering priority [14, 15]. Among the various waste streams contributing to this environmental crisis, end-of-life vehicle tires are considered the most environmentally hazardous wastes, with global production exceeding 1 billion tires annually, while recycling rates remain inadequate [16, 17]. In Algeria, this situation is further exacerbated by the continuous increase in the number of vehicles, generating approximately 45.65 thousand tons of end-of-life tires annually [18], leading to the accumulation of thousands of tons of tires in uncontrolled dumpsites or their open-air incineration, posing a serious threat to public health and the environment.

Concurrently, global plastic production has surpassed 460 million tons per year, contributing substantially to the growing volume of plastic waste, while the quantities accumulating in landfills and aquatic environments threaten fragile ecological systems [19, 20]. The depletion of natural resources, on the one hand, and waste accumulation, on the other, have driven researchers to explore the potential use of these waste materials as reinforcing fibers in concrete within a circular economy framework [21, 22].

Recent studies have revealed that tire-derived steel fibers (TDSF) improve the ductility, tensile strength, and energy absorption capacity of concrete, and possess a unique ability to arrest both micro- and macro-cracks simultaneously, owing to the diversity of their lengths and diameters [23-25]. Furthermore, these fibers reduce the permeability of concrete to chlorides and chemically aggressive agents, which may account for their superior performance compared with commercial fibers in certain chemical deterioration conditions [26, 27]. Waste polyethylene terephthalate (PET) fibers (WPF), on the other hand, have demonstrated notable chemical stability in acidic media, retaining their shape and cross-section without appreciable degradation even after prolonged exposure. They also exhibit the ability to control micro-crack propagation and reduce stress concentrations within the matrix [28, 29].

2. RESEARCH SIGNIFICANCE

Despite the growing interest in the use of TDSF and WPF as sustainable fiber reinforcements in concrete, their effectiveness in improving the chemical durability of SCC under combined aggressive exposure conditions remains insufficiently understood. In particular, limited attention has been given to recycled plastic strapping fibers and to their performance when SCC is simultaneously exposed to acidic and sulfate environments. This represents an important research gap, as such multi-aggressive conditions can induce complex degradation mechanisms that may differ substantially from those observed under single-agent exposure. Addressing this gap is therefore essential for assessing the feasibility of using WPF in SCC designed for demanding and chemically aggressive environments. Accordingly, this study provides a comprehensive experimental investigation of the influence of different fiber contents (0.5–2% by volume) of TDSF and WPF on the chemical resistance of SCC subjected to a combined H_2SO_4, HCl, and Na_2SO_4 attack for 90 and 180 days. The macroscopic deterioration of the mixtures is further correlated with their microstructural characteristics through scanning electron microscopy (SEM) analysis. By simultaneously examining fiber type, fiber dosage, prolonged exposure, multi-aggressive chemical attack, and microstructural evolution, this research provides new insights into the durability potential of WPF in SCC and contributes to the development of more durable and sustainable fiber-reinforced concrete for aggressive service environments. The significance of this study stems from its dual contribution: improving the engineering performance of SCC in aggressive environments, and promoting the valorization of tire and plastic waste within a sustainable development perspective.

3. MATERIALS USED

3.1 Binder system

The binder system consisted of ordinary Portland cement (OPC) CEM I 42.5R, conforming to EN 197-1 standard [30], produced at the Biskra Cement Plant (Algeria), with a specific gravity of 3.20 g/cm³ and a Blaine fineness of 3572 cm²/g. To optimize the packing density of the paste phase and enhance the rheological behavior of the fresh mixtures, a limestone filler (LF) sourced from the Branis quarry (Djamoura, Algeria) was incorporated as a partial powder replacement. The LF exhibited a specific gravity of 2.77 g/cm³ and a high specific surface area of 4500 cm²/g, promoting improved cohesion and reduced bleeding susceptibility in the SCC matrix.

3.2 Aggregates

The granular skeleton consisted of two crushed calcareous coarse aggregate (CA) fractions, namely G1 (4–8 mm with specific gravity of 2.64 g/cm³) and G2 (8–15 mm with specific gravity of 2.68 g/cm³), alongside a crushed calcareous fine aggregate (FA) with specific gravity of 2.61 g/cm³, all sourced from the Ain-Touta quarry (Batna, Algeria) and conforming to the requirements of EN 12620 standard [31].

3.3 Chemical admixture

A third-generation polycarboxylate ether-based superplasticizer (SP), Sika ViscoCrete® Tempo 12 (SIKA), conforming to the NF EN 934-2 standard [32], was incorporated into the SCC mix compositions. The admixture was supplied as a light-to-dark brown liquid, with a pH of 4.5 ± 1 and a density of 1.06 ± 0.01 g/cm³; its chloride ion content was below 0.1%.

3.4 Reinforcing fibers

Three categories of reinforcing fibers were investigated (Figure 1) to assess their comparative effects on the durability of SCC under aggressive chemical exposure: CSF (Cold-drawn collated hooked-end fibers) conforming to the ASTM A820/A820M standard [33], and having a density of 7.8 g/cm³, diameter of 0.54 mm, length of 35 mm, and tensile strength of 1230 MPa. TDSF was recovered from end-of-life passenger vehicle tires and mechanically cleaned before use. They had a density of 6.19 g/cm³, diameter of 0.3 mm, length of 35 ± 5 mm, and tensile strength of 874.16 MPa. WPF was manually extracted from waste PET strapping bands through successive washing, cutting, and drying processes. They had a density of

1.21 g/cm³, diameter of 2 ± 0.5 mm, length of 35 ± 5 mm, and tensile strength of 255 MPa.



Figure 1. Fibers used: (a) waste polyethylene terephthalate (PET) fibers (WPF), (b) tire-derived steel fibers (TDSF), (c) conventional steel fibers (CSF)

4. MIX DESIGN AND EXPERIMENTAL PROGRAM

The SCC mixtures were designed using a volumetric approach to ensure a total fresh concrete volume of 1 m^3. The mix design was governed by the following key parameters, selected based on rheological compatibility and optimized paste-to-aggregate balance: a water-to-binder ratio of 0.41, a cement content of 420 kg/m^3, LF content of 74 kg/m^3, SP content of 1.60%, and a CA-to-FA ratio of 1. Fiber reinforcement was introduced at four volume fractions (0.5%, 1.0%, 1.5%, and 2.0%) by volumetrically replacing an equivalent portion of the aggregate skeleton, thereby maintaining a constant total mixture volume.

Cubic specimens measuring 100 × 100 × 100 mm were cast from each SCC mixture without mechanical vibration. After demolding at 24 h, all specimens were water-cured at 20 ± 2 °C for 28 days in accordance with EN 12390-2 standard [34], to ensure sufficient hydration before exposure to the chemical solutions.

Upon completion of the curing period, the specimens were fully immersed in three chemically aggressive solutions, representing major environmental and industrial deterioration scenarios encountered in practice: HCl at a concentration of 5%, simulating acidic industrial effluents, chemical processing environments, and microbially induced corrosion in sewer systems. H_2SO_4 at a concentration of 5%, representing the most deleterious acid attack mechanism for cementitious composites, leading to progressive decalcification, gypsum crystallization, and ettringite-induced expansion. Na_2SO_4 at 50 g/L: conforming to the concentration prescribed by the ASTM C1012/C1012M standard [35], simulating sulfate-laden groundwater and aggressive soil conditions. It should be noted that a 5% concentration was adopted to represent severe acidic exposure conditions and to enable a clear assessment of the deterioration mechanisms associated with hydrochloric and sulfuric acid attack.

All specimens were maintained at ambient laboratory temperature throughout the immersion period. The solutions were completely renewed every two weeks to maintain their chemical aggressiveness and prevent progressive neutralization. The pH of each solution was monitored at regular intervals using a calibrated digital pH meter to provide a continuous indication of solution stability. Exposure periods of 90 and 180 days were selected to capture the time-dependent progression of chemical degradation [36].

Mass loss and compressive strength loss tests were carried out according to ASTM C267 [37] and EN 12390-3 standards [38], respectively. Each obtained result represents the average of three readings (Figure 2). Furthermore, SEM was carried out on specimens to provide qualitative insight into the microstructural changes induced by chemical exposure [39]. Representative SCC fragments were collected from the tested specimens after the designated exposure periods. The samples were carefully extracted from the interior of the specimens to minimize the influence of surface deterioration and to obtain representative portions of the concrete matrix. The selected fragments were gently rinsed to remove loose surface deposits and were subsequently dried to eliminate residual moisture. The dried specimens were then cut into small pieces of suitable dimensions for SEM observation. The surfaces intended for microscopic examination were carefully prepared to obtain a relatively smooth and clean surface while minimizing mechanical damage to the cementitious matrix. Before SEM examination, the specimens were mounted on aluminum stubs using conductive carbon tape and coated with a thin conductive layer to prevent charging under the electron beam. The prepared samples were then examined using an SEM to characterize the microstructural features of the cement matrix, including hydration products, pores, microcracks, fibers, and deterioration products formed as a result of chemical exposure.

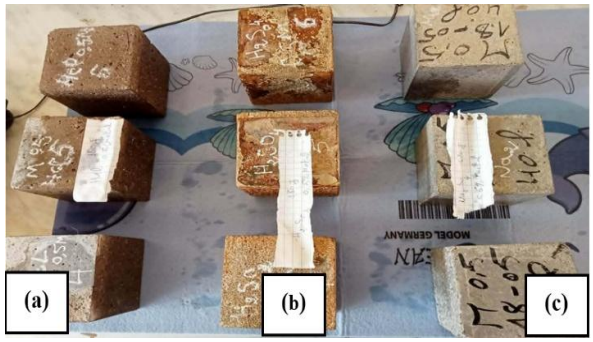


Figure 2. Samples' state after exposure to aggressive environments: (a) HCl, (b) H_2SO_4, (c) Na_2SO_4

5. RESULTS AND DISCUSSION

5.1 Mass loss under HCl acid

Figure 3 presents the evolution of mass loss in the SCC mixtures in HCl solution after 90 and 180 days. All mixtures exhibited a gradual increase in mass loss with increasing exposure duration. The M-Ref mixture showed relatively limited mass loss of 1.18% and 1.52% after 90 and 180 days, respectively, due to the dissolution of hydration products such as $Ca(OH)_2$ and C-S-H gel, and decalcification, as described by Eq. (1).

$$Ca(OH)_2 + 2HCl \rightarrow CaCl_2 + 2H_2O \quad (1)$$

Acid attack causes decalcification of C-S-H, resulting in calcium leaching and the formation of silica-rich residues.

This process results in the formation of highly soluble calcium chloride ($CaCl_2$) that is readily leached out of the matrix. This finding is consistent with the result reported by Siad et al. [40], who demonstrated that acid attack targets calcareous compounds, leading to a reduction in durability. In contrast, CSF-reinforced SCC exhibited more severe degradation. The mass loss in the M-CSF2 mixture reached its highest value of 5.81% and 8.47% after 90 and 180 days, respectively. This is attributed to the combined effect of acid

attack and the corrosion and dissolution of iron (Fe) within the cracks, as described by Eq. (2).

$$Fe + 2HCl \rightarrow FeCl_2 + H_2\uparrow \quad (2)$$

H_2 generates internal stresses that accelerate matrix decomposition [41].

While SCC reinforced with 2%TDSF exhibited significant mass losses of 4.44% and 5.50% after 90 and 180 days, respectively, its performance remained superior to CSF. This is attributed to the properties of TDSF, whereby residual coatings or surface rubber impurities provide temporary physical protection that delays acid penetration and subsequent attack of the steel, confirming that TDSF can perform as well as, or even better than, CSF in aggressive chemical environments [42, 43]. On the other hand, mixtures reinforced with WPF demonstrated the highest resistance to acid attack. Mixture M-WPF2 exhibited the lowest mass loss of 0.23% and 0.30% at 90 and 180 days, respectively, corresponding to an approximately 80.26% reduction compared to the M-Ref mixture. This is attributed to the superior performance resulting from the chemical stability and acid inertness of WPF, in addition to their role in reducing the permeability of aggressive agents and increasing the tortuosity of the transport paths within the matrix [44].

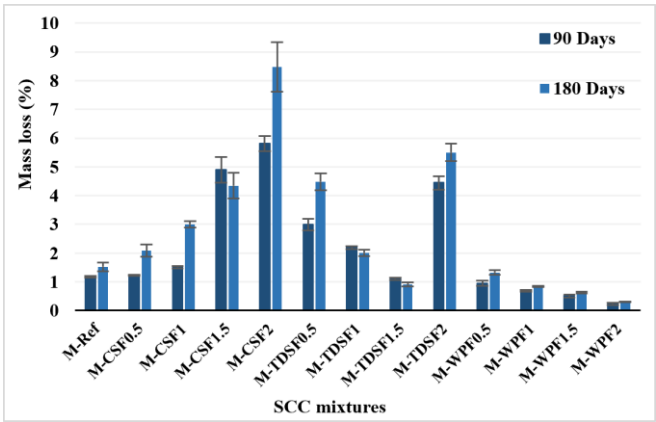


Figure 3. Mass loss of self-compacting concrete (SCC) mixes under HCl acid

5.2 Compressive strength loss under HCl acid

Figure 4 illustrates the evolution of compressive strength loss in SCC mixtures exposed to a 5% HCl solution for 90 and 180 days. For all mixes, compressive strength loss increased significantly with exposure duration, indicating a gradual deterioration of the cementitious matrix. HCl attacks the reaction products responsible for strength development, particularly C-S-H, leading to decalcification, increased porosity, and microcrack formation. As the exposure period increased from 90 to 180 days, the acid penetration front advanced deeper into the matrix, causing a significant decrease in the effective cross-sectional area available to resist compressive loads [45-48].

The M-Ref mixture exhibited a compressive strength loss of 13.81% after 180 days. This loss can be attributed to the progressive dissolution and degradation of C-S-H and portlandite, resulting in the severe deterioration of the cementitious matrix. CSF-reinforced SCC showed the highest loss in compressive strength, with the M-CSF2 mixture showing a decrease of 24.92%. Youssari et al. [41] showed that acidic environments accelerate leaching and deterioration of the ITZ, reducing the efficiency of stress transfer between the CSF and the surrounding matrix [49-51]. Exposure of M-TDSF mixtures to HCl resulted in the deterioration of both the cementitious matrix and the fiber-matrix interface. However, the presence of rubber residues adhering to TDSF reduced the rate of degradation compared with CSF. Su et al. [52] confirmed that these fibers improve toughness and mitigate stiffness and strength loss during chemical attack due to their crack-bridging ability [53, 54]. The M-WPF mixtures exhibited the lowest compressive strength losses among all fiber-reinforced SCC mixtures. Specifically, the M-WPF2 mix showed losses of only 12.60% after 180 days. This outstanding performance is attributed to the chemical inertness of the plastic fibers, which exhibit high resistance to HCl exposure and thus retain their strengthening function throughout the exposure period [44, 55, 56].

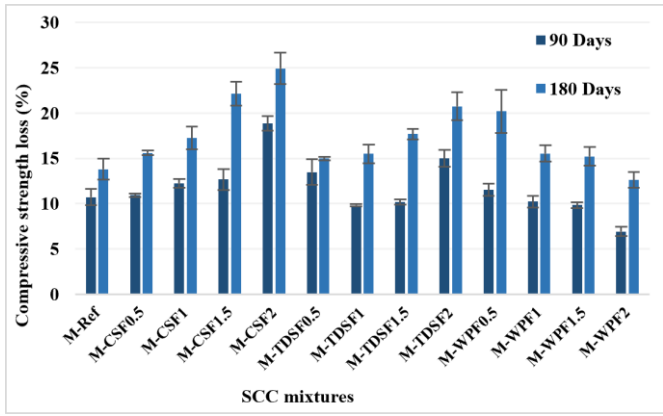


Figure 4. Compressive strength loss of self-compacting concrete (SCC) mixes under HCl acid

5.3 Mass loss under H_2SO_4 solution

Figure 5 shows the mass loss results for the SCC mixtures exposed to H_2SO_4 solution. A clear variation in mass loss behavior depending on the fiber type, dosage, and exposure duration was observed. The M-Ref mixture exhibited mass losses of 0.93% and 0.98% at 90 and 180 days, respectively, indicating a nearly constant and non-accelerating rate of surface degradation over time. From a chemical perspective, this overall behavior remains governed by the fundamental reactions presented in Eqs. (3) and (4).

$$Ca(OH)_2 + H_2SO_4 \rightarrow CaSO_4 + 2H_2O \quad (3)$$

$$CaCO_3 + H_2SO_4 \rightarrow CaSO_4 + CO_2 + H_2O \quad (4)$$

M-CSF mixtures exhibited a sharp increase in mass loss, with the highest values reaching 4.46% and 3.70% in the M-CSF2 mixture at 90 and 180 days, respectively. The convergence of the differences between the two exposure periods in the higher-dose mixture suggests that surface degradation reached a point of saturation where the most vulnerable layers had already flaked off, rather than indicating a genuine increase in resistance [9]. Aslani et al. [57] attributed this loss of mass to the effect of excessive addition of CSF, which disrupts the self-compacting mechanism, promotes fiber agglomeration, and facilitates acid penetration into the damaged internal structure. In contrast, M-TDSF showed better performance compared to M-CSF under H_2SO_4

exposure, particularly at low fiber dosages. With the addition of 0.5%TDSF, mass loss was limited to 0.45% after 180 days, compared to 1.13% for the M-CSF 0.5 mixture. Mass loss gradually increased to 1.48% for M-TDSF2 and to 3.7% for M-CSF2% after 180 days. Hichem et al. [58] and Yu et al. [59] indicated that TDSF fibers successfully limit the accumulation of long-term deterioration and delay surface scaling by enhancing mechanical bonding and scaling resistance through their irregular surface roughness, consistently outperforming reference concrete. However, a significant increase in TDSF content may increase porosity and facilitate ion penetration.

Meanwhile, M-WPF mixtures exhibited a fluctuating but downward trend in mass loss with increasing fiber dosage, reaching 1.28% and 0.35% for M-WPF0.5 and M-WPF2 mixtures, respectively, after 180 days. This trend can be attributed to the chemical inertness of WPF, as reported by Prasad and Goud [44]. The chemical inertness of WPF helps protect the surface from direct acid attack and limit mass loss; however, it may also result in a weak interface with the matrix, which becomes a preferential pathway for internal acid penetration and accelerates structural deterioration.

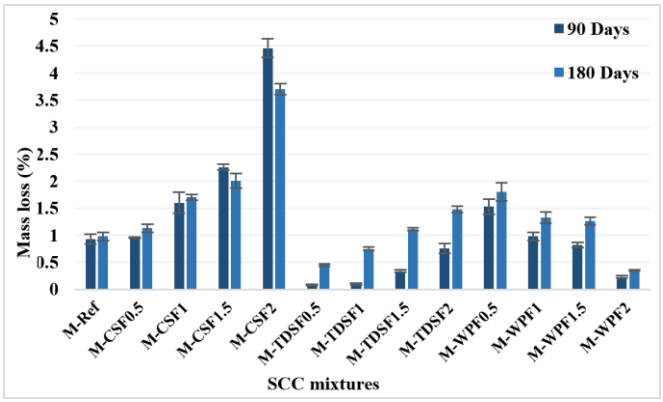


Figure 5. Mass loss of self-compacting concrete (SCC) mixes under H_2SO_4 solution

5.4 Compressive strength loss under H_2SO_4 solution

The strength loss shown in Figure 6 indicates that the M-Ref mixture experienced losses of 8.50% and 13.73% after 90 and 180 days, respectively, demonstrating the gradual accumulation of structural deterioration in the fiber-free reference matrix. The M-CSF mixtures exhibited a clear upward trend with increasing content, reaching a maximum of 26.93% for the M-CSF2 mixture after 180 days. This reflects the formation of gypsum crystals at the fiber-matrix interface and their subsequent dispersion throughout the cementitious matrix [60, 61]. These crystals weaken the surface layer and gradually weaken the fiber-matrix bond. Awrahman et al. [9] noted that exceeding the optimum ratio disrupts the self-compacting mechanism and creates additional pathways for acid penetration. In contrast, the M-TDSF mixtures achieved the best overall performance, with M-TDSF0.5 recording the lowest strength loss of 6.96% after 180 days. This favorable behavior was most evident at fiber contents up to 1%, beyond which the improvement became less pronounced. The residual surface protection provided by TDSF can help restrict the propagation of internal load-bearing cracks and delay acid penetration into the core of the matrix [59]. Zia et al. [62] confirmed that a high TDSF content can increase internal porosity due to agglomeration, thereby reducing the chemical resistance of concrete. M-WPF mixtures, on the other hand, showed the highest progressive increase in resistance loss with increasing content. M-WPF2 mixture reached the highest value with a sharp loss of 42.67%. Chen et al. [63] attributed this behavior to the loss of effectiveness of plastic fibers at high doses because of air entrapment and a weakened interfacial surface, which becomes a preferred pathway for H_2SO_4 penetration [64].

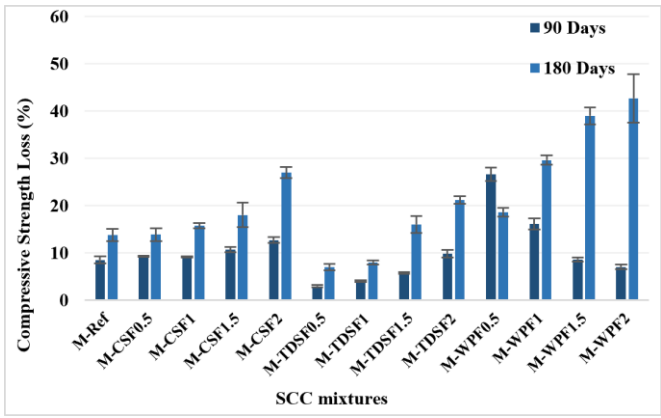


Figure 6. Compressive strength loss of self-compacting concrete (SCC) mixes under H_2SO_4 solution

5.5 Mass loss under Na_2SO_4 solution

The mass loss results for the SCC mixtures exposed to the Na_2SO_4 solution are shown in Figure 7. A marked difference between the behavior of specimens exposed to Na_2SO_4 and that of specimens immersed in H_2SO_4 or HCl can be observed. According to Eqs. (5)-(7), a coupled chemical–physical mechanism leads to the formation of gypsum and ettringite-related products, which first fill larger voids, transforming them into smaller- and medium-sized pores, thus increasing density and mass, as reflected by the negative mass-loss values. Then, with continued exposure, the available void space becomes progressively saturated, and expansion stresses begin to generate new cracks that dislodge matrix material, ultimately resulting in a positive mass loss [65-67].

$$Ca(OH)_2 + Na_2SO_4 + 2H_2O \rightarrow CaSO_4 \cdot 2H_2O + 2NaOH \quad (5)$$

$$Ca_3A + 3(CaSO_4 + 2H_2O) + 26H_2O \rightarrow Ca_6AS_3H_{33} \quad (6)$$

$$Na_2SO_4 + 10H_2O \rightarrow Na_2SO_4 + 10H_2O \quad (7)$$

The M-Ref mixture exhibited a mass gain of 0.21% and 0.25% after 90 and 180 days, respectively. This reflects the absence of any factor restricting SO_4^{2-} penetration, allowing the reaction products to freely enter the matrix without yet reaching the point at which the available void space is exceeded [65-67].

It can also be observed that, except for M-WPF, all mixtures exhibited a direct relationship between increasing fiber content and increasing mass loss at 180 days. This indicates that higher fiber reinforcement is associated with increased actual mass loss over extended exposure. For M-CSF mixtures, at 90 days, the values ranged from −0.23% for M-CSF0.5, indicating mass gain, to −0.12% for both M-CSF1.5 and M-CSF2. However, this trend changed markedly after 180 days. M-CSF1.5 and M-CSF2 exhibited mass losses of 1.14% and

1.63%, respectively, with M-CSF2 recording the highest actual mass loss in the entire experimental program. Marrok et al. [64] demonstrated that CSF provides mechanical anchoring sites that increase the internal retention of reaction products and amplify the volumetric confinement effect as the fiber content increases. This perfectly matches the initial phase recorded at 90 days, while the subsequent reversal to +1.63% at 180 days reflects the exceedance of the retention capacity and the onset of matrix material loss due to cracks resulting from accumulated expansion stress. Also, the M-TDSF mixtures exhibited relatively stable mass-change behavior, although M-TDSF1 showed a distinct deviation from the general trend. M-TDSF1 recorded a mass gain of 0.34% at 90 days, representing the highest mass gain in the experimental program, which decreased to 0.13% at 180 days. In contrast, M-TDSF1.5 and M-TDSF2 exhibited progressively increasing mass losses, from 0.18% to 0.36% and from 0.50% to 0.70%, respectively. Althoey et al. [27] reported that TDSF may improve sulfate resistance and promote a more uniform distribution of internal stresses because of their irregular geometry and rough surface. This behavior explains the relatively consistent response of M-TDSF0.5, M-TDSF1.5, and M-TDSF2. However, the reduced mass gain observed for M-TDSF1 may indicate localized microcracking or the partial release of previously retained sulfate reaction products before the system reached a stable condition. Finally, the M-WPF mixtures exhibited the narrowest range of mass-change values between 90 and 180 days. M-WPF0.5 recorded a mass loss of only 0.004% after 90 days, representing the lowest loss among all mixtures. After 180 days, mass loss increased gradually from 0.073% to 0.16% with increasing WPF content. This stable behavior may be attributed to the chemical inertness of WPF and its role in limiting the continuity of transport pathways within the cementitious matrix. Liu et al. [68] reported that plastic fibers can improve pore-size distribution and restrict the ingress of aggressive ions, thereby slowing sulfate-related reactions. Moreover, Lu et al. [69] showed that plastic fibers can mitigate the development of localized internal stress concentrations within the cementitious matrix. This mechanism may explain the stable mass response and the absence of sharp transitions between the accumulation and release of reaction products.

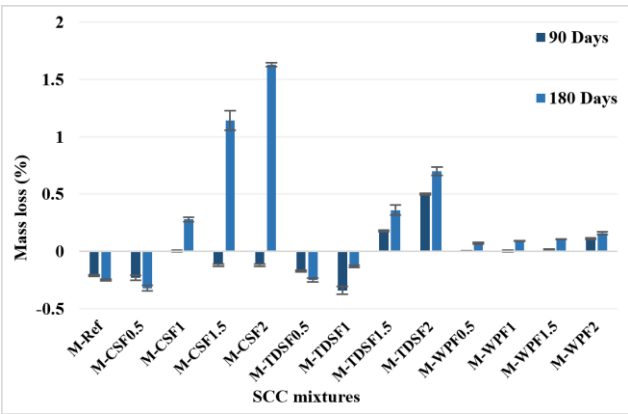


Figure 7. Mass loss of self-compacting concrete (SCC) mixes under Na_2SO_4 Solution

5.6 Compressive strength loss under Na_2SO_4 solution

Compressive strength provides an indication of whether the cementitious structure undergoes consolidation or deterioration. Under Na_2SO_4 exposure, SO_4^{2-} first reacts with $Ca(OH)_2$ to form gypsum, filling large voids, then with free C_3A to form ettringite, closing remaining voids (Eqs. (5)-(6)), thereby contributing to an early increase in compressive strength. Guo et al. [70] linked this directly to the strength increase observed in M-WPF mixtures at 90 days. Once ettringite accumulation exceeds pore capacity, this initial strength gain is reversed, leading to a sharp loss in strength, as expansion stress exceeds tensile strength and accelerates SO_4^{2-} penetration into its interior. Biscaro et al. [71] showed this manifests as "onion-peel" cracking from the surface inward, and the presence of fibers contributes to stress redistribution and limits internal crack development. In addition to these mechanisms, the decalcification of the C-S-H phase (Eq. (8)) provides a complementary explanation for the time-dependent acceleration of strength loss. This mechanism should therefore be considered alongside the processes discussed in the mass-loss analysis, without excluding the potential contribution of mirabilite formation to the strength response.

$$NaOH + C\text{-}S\text{-}H \rightarrow Na_2SiO_3 + Ca(OH)_2 + H_2O \quad (8)$$

Decalcification of the C-S-H phase regenerates $Ca(OH)_2$, feeding back into the initial reaction pathway and forming a self-sustaining cycle that explains accelerated degradation between 90 and 180 days. Guo et al. [70] documented this cycle in advanced exposure stages.

Figure 8 shows that M-Ref compressive strength loss rose from 11.34% at 90 days to 22.5% at 180 days. In contrast, the M-CSF mixtures exhibited a decrease in compressive strength loss with increasing CSF content, with the M-CSF2 mixture showing the lowest loss, at 7.65%. This behavior is attributed to the fact that, at lower CSF content, fibers cannot form a sufficiently strong network to restrain ettringite stresses, accelerating deterioration past tensile strength, but at higher CSF contents, a dense fiber network restrains crack development [70]. It should be noted that M-CSF2 recorded the highest mass loss under Na_2SO_4. This apparent contradiction can be explained by the ability of CSF to temporarily retain the deteriorated matrix components, thereby delaying structural collapse while allowing expansive reaction products to accumulate. Once the resulting internal stresses exceeded the material's load-bearing capacity, surface flaking occurred [72].

M-TDSF mixtures generally exhibited similar behavior to M-CSF mixtures, where compressive strength loss decreases with increasing TDSF content. M-TDSF1.5 recorded the lowest loss of 4.96 at 180 days. Qin et al. [73] noted that TDSF with a rough surface retained 87% of the ITZ interfacial strength after 90 days in Na_2SO_4 compared to only 61% for fine fibers, which may explain the long-term relative superiority. Ran et al. [74] reported that excessive fiber content can adversely affect strength despite generally inhibiting microcracks. This may explain the increase in compressive strength loss observed for M-TDSF2.

M-WPF mixtures showed a unique characteristic. In fact, M-WPF0.5 showed an increase in compressive strength loss from 6.4% at 90 days to 11.22% at 180 days. In contrast, the other three mixtures initially exhibited compressive strength gains after 90 days before transitioning to strength losses after 180 days. For example, the M-WPF2 mixture exhibited a compressive strength gain of 8.13% at 90 days, followed by a loss at 180 days of 1.70%. It should be noted that M-WPF exhibited the lowest compressive strength losses compared

with the other fiber types used. This is attributed to the chemical inertness of WPF [72, 75].

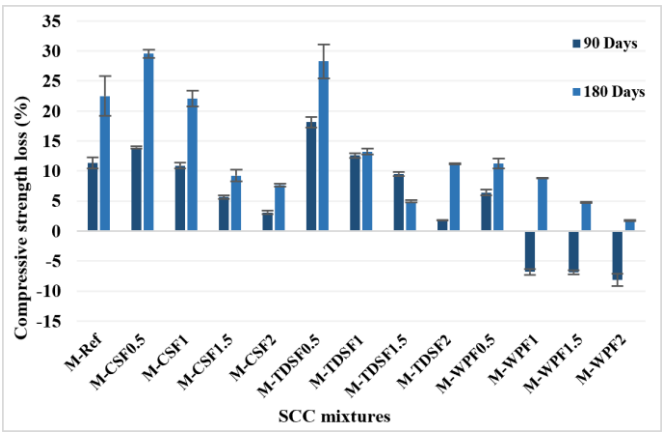
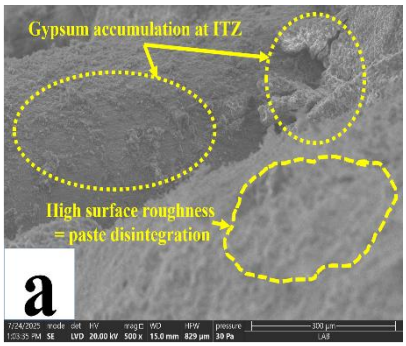


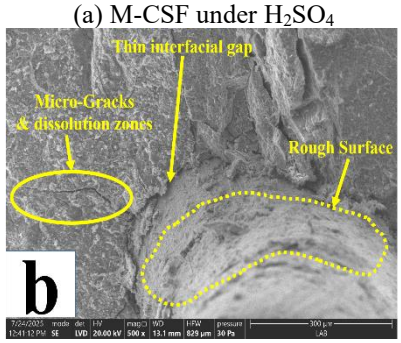
Figure 8. Compressive strength loss of self-compacting concrete (SCC) mixes after exposure to Na_2SO_4 solution

5.7 Scanning electron microscopy analysis of self-compacting concrete under chemical attack

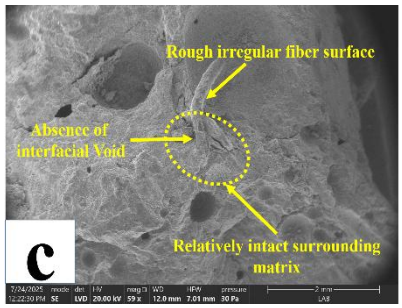
Figure 9 presents microscopic images of the samples after exposure to H_2SO_4, HCl, and Na_2SO_4 media. Figure 9(a) reveals the formation and dispersion of oval-shaped gypsum crystals in the cementitious paste surrounding the CSF fibers under H_2SO_4 attack, providing direct microscopic evidence of the localized interaction between the acidic medium and the C-S-H gel within the ITZ and its progressive degradation [60]. This observation is consistent with the highest compressive strength loss recorded in this class. Under HCl attack, Figure 9(b) shows a pattern similar to that of the same fiber type: the dissolution of portlandite and C-S-H gel decalcification lead to increased local porosity and the formation of microcracks around the fibers [76]. These observations provide visual evidence consistent with the sharp loss of resistance, which reached 24.92% in the M-CSF2 mixture under this medium.



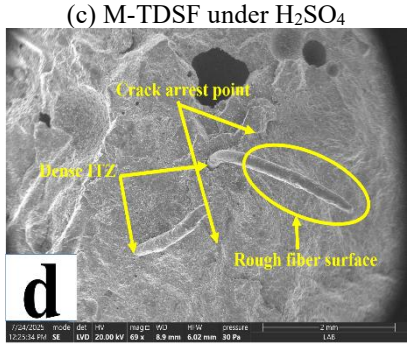
(a) M-CSF under H_2SO_4



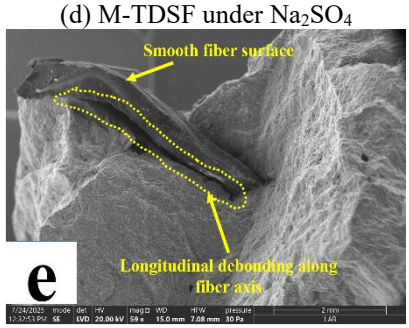
(b) M-CSF under HCl



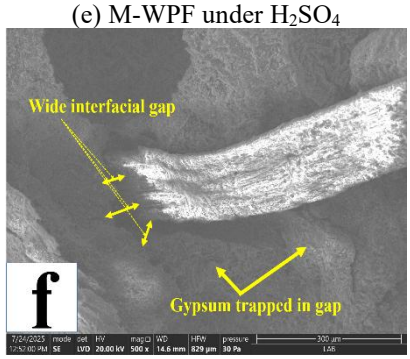
(c) M-TDSF under H_2SO_4



(d) M-TDSF under Na_2SO_4



(e) M-WPF under H_2SO_4



(f) M-WPF under Na_2SO_4

Figure 9. Scanning electron microscopy (SEM) morphology of mixture degradation

TDSF consistently exhibits a crack-arresting mechanism regardless of the aggressive medium. Figure 9(c), obtained after H_2SO_4 exposure, clearly shows the microcracks stopping at the fiber boundary and failing to propagate through the surrounding matrix, providing a direct microscopic embodiment of the crack-arresting mechanism, with a rough fiber surface, which promotes stronger bonding to the paste [24, 77]. This microscopic mechanism is what explains the M-TDSF0.5 mixture registering the lowest compressive strength loss. This protective behavior is repeated under Na_2SO_4 exposure. Figure 9(d) shows a clear crack-arresting point at the fiber boundary with a dense ITZ and a rough fiber surface [24], accurately reflecting a deep protective mechanism that parallels the remarkable resistive stability and initial strength gain noted in M-TDSF1.5 and M-TDSF2 mixtures under this medium. In contrast, WPF exhibits a distinctly different and

medium-dependent behavior on the chemical nature of the aggressive medium. Figure 9(e) shows, under H_2SO_4, large interfacial voids surrounding the smooth WPF fibers, with no visible adhering residues, evidence that an effective fiber–matrix bond was not fully established, making this gap a preferential pathway for acid penetration [46, 63]. This observation is consistent with the highest compressive strength loss recorded under H_2SO_4. Notably, under Na_2SO_4 attack, this structural void appears to serve a different function. Figure 9(f) reveals a large interfacial gap that confines gypsum and secondary ettringite, isolated from the surrounding matrix rather than uniformly distributed within it [72, 78]. This is direct visual evidence explaining the pronounced fluctuations in compressive strength noted in M-WPF mixtures under sulfate exposure, despite the minimal mass change recorded in this class. This reversal confirms that the identical interfacial geometry can act either as a destructive attack channel or a temporary reservoir for reaction products, depending on the ionic species present in the surrounding environment.

6. CONCLUSIONS

This study evaluated the durability of SCC reinforced with 0.5%, 1%, 1.5%, and 2% of CSF, TDSF, and WPF under exposure to HCl, H_2SO_4, and Na_2SO_4 solutions over periods of 90 and 180 days. Based on the results obtained, the following key points can be drawn:

•Regarding mass loss under chemical exposure, WPF-reinforced SCC demonstrated the greatest resistance due to the chemical inertness of WPF. TDSF-reinforced SCC ranked second, as the residual rubber layer on the fiber surface provided temporary physical protection against acid attack. Conversely, CSF-reinforced SCC exhibited the poorest mass loss resistance because CSF underwent corrosion and degradation in acidic environments, thereby accelerating the deterioration of the composite.

•Regarding compressive strength loss, TDSF-reinforced SCC consistently outperformed CSF-reinforced SCC regardless of the type of acid used. In contrast, the effectiveness of WPF depended on the exposure medium. Specifically, under HCl and Na_2SO_4 exposure, WPF-reinforced SCC exhibited the highest resistance to compressive strength degradation among the investigated fiber systems. However, under H_2SO_4 exposure, WPF-reinforced SCC showed the lowest resistance, indicating that its performance is strongly dependent on the chemical environment.

•The optimal fiber type and dosage for enhancing durability cannot be universally defined but must be carefully tailored to the specific chemical exposure conditions. Under H_2SO_4 exposure, a low TDSF dosage of 0.5% is recommended to minimize compressive strength loss. In contrast, under HCl and Na_2SO_4 exposure, a higher WPF dosage of 2% was found to be optimal, providing the greatest resistance to compressive strength degradation.

•Microscopic analysis using SEM clearly confirmed these macroscopic findings. CSF showed gypsum crystal accumulation and C-S-H gel degradation at the interface, while TDSF demonstrated a clear cessation of cracking at the fiber boundary with strong mechanical bonding due to its rough surface. WPF, on the other hand, displayed a wide interfacial gap around the fiber, alternating between a protective insulating role in HCl and Na_2SO_4 and a destructive role as an acid penetration pathway in H_2SO_4.

ACKNOWLEDGMENT

The authors gratefully acknowledge the technical support provided by the Mining Laboratory of the University of Echahid Cheikh Larbi Tebessi and the Construction Materials Laboratory of the University of Mohamed Khider.

REFERENCES

[1] Okamura, H., Ouchi, M. (2003). Self-compacting concrete. Journal of Advanced Concrete Technology, 1(1): 5-15. https://doi.org/10.3151/jact.1.5

[2] Okamura, H., Ouchi, M. (1998). Self-compacting high performance concrete. Progress in Structural Engineering and Materials, 1(4): 378-383. https://doi.org/10.1002/pse.2260010406

[3] Bouabdallah, M.A. (2025). The impact of admixtures on the rheological properties of self-compacting concrete with and without fly ash: A review. Journal of Building Materials and Structures, 12(2): 145-169. https://doi.org/10.34118/jbms.v12i2.4332

[4] Athiyamaan, V., Ganesh, G.M. (2017). Statistical and detailed analysis on fiber reinforced self-compacting concrete containing admixtures: A state of art of review. IOP Conference Series: Materials Science and Engineering, 263: 032037. https://doi.org/10.1088/1757-899x/263/3/032037

[5] Irico, S., De Meyst, L., Qvaeschning, D., Alonso, M.C., Villar, K., De Belie, N. (2020). Severe sulfuric acid attack on self-compacting concrete with granulometrically optimized blast-furnace slag: Comparison of different test methods. Materials, 13(6): 1431. https://doi.org/10.3390/ma13061431

[6] Ferrari, C., Puglia, M., Morselli, N., et al. (2025). Characterization and durability of cool materials: Standard methodologies for the evaluation of thermal performance of new and aged products. Power Engineering and Engineering Thermophysics, 4(3): 160-167. https://doi.org/10.56578/peet040302

[7] Zhang, C., Li, J., Yu, M., Lu, Y., Liu, S. (2024). Mechanism and performance control methods of sulfate attack on concrete: A review. Materials, 17(19): 4836. https://doi.org/10.3390/ma17194836

[8] Boughamsa, O., Abdelouahed, A., Hebhoub, H., Kherraf, L., Boukhatem, G. (2023). Optimizing sand concrete properties through partial substitution of natural sand with cement kiln dust. Annales de Chimie - Science des Matériaux, 47(4): 259-264. https://doi.org/10.18280/acsm.470408

[9] Awrahman, A.H., Eren, N.A., Çevik, A., Mohammed, A.A. (2023). Experimental study on direct shear strength of fiber reinforced self compacting concrete under acid and sulfate attack. Periodica Polytechnica Civil Engineering, 68(2): 392-402. https://doi.org/10.3311/ppci.22519

[10] Talaeitaba, S.B., Masoomi, R., Behravan, A., Razavi, M. (2026). Forta and steel fiber reinforced lightweight self-compacted concrete: Mechanical properties and durability in sulfate, acid and chloride attack. International Journal of Concrete Structures and

Materials, 20: 6. https://doi.org/10.1186/s40069-025-00845-6
[11] Yu, J., Qiao, H., Zhu, F., Wang, X. (2021). Research on damage and deterioration of fiber concrete under acid rain environment based on GM(1,1)-Markov. Materials, 14(21): 6326. https://doi.org/10.3390/ma14216326
[12] Ji, Y., Xu, W., Sun, Y., Ma, Y., He, Q., Xing, Z. (2022). Grey correlation analysis of the durability of steel fiber-reinforced concrete under environmental action. Materials, 15(14): 4748. https://doi.org/10.3390/ma15144748
[13] Kos, Ž., Kroviakov, S., Kryzhanovskyi, V., Hedulian, D. (2022). Strength, frost resistance, and resistance to acid attacks on fiber-reinforced concrete for industrial floors and road pavements with steel and polypropylene fibers. Materials, 15(23): 8339. https://doi.org/10.3390/ma15238339
[14] Olsson, J.A., Miller, S.A., Alexander, M.G. (2023). Near-term pathways for decarbonizing global concrete production. Nature Communications, 14: 4574. https://doi.org/10.1038/s41467-023-40302-0
[15] Collivignarelli, M.C., Cillari, G., Ricciardi, P., et al. (2020). The production of sustainable concrete with the use of alternative aggregates: A review. Sustainability, 12(19): 7903. https://doi.org/10.3390/su12197903
[16] Czarna-Juszkiewicz, D., Kunecki, P., Cader, J., Wdowin, M. (2023). Review in waste tire management: Potential applications in mitigating environmental pollution. Materials, 16(17): 5771. https://doi.org/10.3390/ma16175771
[17] Hashamfirooz, M., Dehghani, M.H., Khanizadeh, M., et al. (2025). A systematic review of the environmental and health effects of waste tires recycling. Heliyon, 11(2): e41909. https://doi.org/10.1016/j.heliyon.2025.e41909
[18] Djebien, R., Bouabaz, A., Abbas, Y. (2022). Effect of recycled tire rubber and marble waste on fresh and hardened properties of concrete. Civil and Environmental Engineering Reports, 32(1): 218-239. https://doi.org/10.2478/ceer-2022-0013
[19] Enache, A.C., Grecu, I., Samoila, P. (2024). Polyethylene terephthalate (PET) recycled by catalytic glycolysis: A bridge toward circular economy principles. Materials, 17(12): 2991. https://doi.org/10.3390/ma17122991
[20] Duan, C., Wang, Z., Zhou, B., Yao, X. (2024). Global polyethylene terephthalate (PET) plastic supply chain resource metabolism efficiency and carbon emissions co-reduction strategies. Sustainability, 16(10): 3926. https://doi.org/10.3390/su16103926
[21] Minde, P., Kulkarni, M., Patil, J., Shelake, A. (2024). Comprehensive review on the use of plastic waste in sustainable concrete construction. Discover Materials, 4: 58. https://doi.org/10.1007/s43939-024-00126-1
[22] Saha, S., Sau, D., Hazra, T. (2023). Economic viability analysis of recycling waste plastic as aggregates in green sustainable concrete. Waste Management, 169: 289-300. https://doi.org/10.1016/j.wasman.2023.07.023
[23] Pawelska-Mazur, M., Kaszynska, M. (2021). Mechanical performance and environmental assessment of sustainable concrete reinforced with recycled end-of-life tyre fibres. Materials, 14(2): 256. https://doi.org/10.3390/ma14020256
[24] Michalik, A., Chyliński, F., Bobrowicz, J., Pichór, W. (2022). Effectiveness of concrete reinforcement with recycled tyre steel fibres. Materials, 15(7): 2444. https://doi.org/10.3390/ma15072444
[25] Othman, P.M., Herki, B.M.A. (2026). Evaluation of the resistance of concrete to freezing and thawing containing recycled steel fibers and waste aluminum aggregates. Journal of Composites Science, 10(4): 183. https://doi.org/10.3390/jcs10040183
[26] Augustino, D.S., Onchiri, R.O., Kabubo, C., Kanali, C. (2022). Mechanical and durability performance of high-strength concrete with waste tyre steel fibres. Advances in Civil Engineering, 2022(1): 4691972. https://doi.org/10.1155/2022/4691972
[27] Althoey, F., Zaid, O., Mohamed Elhadi, K. (2024). Correction: Sulfate activation of wheat straw ash to enhance the properties of high-performance concrete with recycled aggregates and waste tire steel fibers. PLoS ONE, 19(12): e0316659. https://doi.org/10.1371/journal.pone.0316659
[28] Pelisser, F., Montedo, O.R.K., Gleize, P.J.P., Roman, H.R. (2012). Mechanical properties of recycled PET fibers in concrete. Materials Research, 15(4): 679-686. https://doi.org/10.1590/s1516-14392012005000088
[29] Meza, A., Pujadas, P., Meza, L.M., Pardo-Bosch, F., López-Carreño, R.D. (2021). Mechanical optimization of concrete with recycled PET fibres based on a statistical-experimental study. Materials, 14(2): 240. https://doi.org/10.3390/ma14020240
[30] European Committee for Standardization. (2011). EN 197-1:2011: Cement — Part 1: Composition, specifications and conformity criteria for common cements.
[31] European Committee for Standardization. (2013). EN 12620:2013: Aggregates for concrete.
[32] European Committee for Standardization. (2012). EN 934-2:2009+A1:2012: Admixtures for concrete, mortar and grout - Part 2: Concrete admixtures - Definitions, requirements, conformity, marking and labelling.
[33] ASTM International. (2016). ASTM A820-01: Standard specification for steel fibers for fiber-reinforced concrete. https://doi.org/10.1520/A0820-01
[34] European Committee for Standardization. (2019). EN 12390-2:2019: Testing hardened concrete — Part 2: Making and curing specimens for strength tests.
[35] ASTM International. (2018). ASTM C1012/C1012M-18b: Standard test method for length change of hydraulic-cement mortars exposed to a sulfate solution. https://doi.org/10.1520/C1012_C1012M-18B
[36] Dansk Standard. (2021). DS/EN 206:2013+A2:2021: Concrete — Specification, performance, production and conformity.
[37] ASTM International. (2012). ASTM C267-01: Standard test methods for chemical resistance of mortars, grouts, and monolithic surfacings and polymer concretes. https://doi.org/10.1520/C0267-01
[38] European Committee for Standardization. (2019). EN 12390-3:2019: Testing hardened concrete - Part 3: Compressive strength of test specimens.
[39] ASTM International. (2022). ASTM C1723-16: Standard guide for examination of hardened concrete using scanning electron microscopy. https://doi.org/10.1520/C1723-16R22
[40] Siad, H., Mesbah, H.A., Khelafi, H., Kamali-Bernard, S., Mouli, M. (2010). Effect of mineral admixture on resistance to sulphuric and hydrochloric acid attacks in

self-compacting concrete. Canadian Journal of Civil Engineering, 37(3): 441-449. https://doi.org/10.1139/l09-157
[41] Youssari, F.Z., Taleb, O., Benosman, A.S. (2023). Towards understanding the behavior of fiber-reinforced concrete in aggressive environments: Acid attacks and leaching. Construction and Building Materials, 368: 130444. https://doi.org/10.1016/j.conbuildmat.2023.130444
[42] Abdolpour, H., Niewiadomski, P., Sadowski, Ł., Kwiecień, A. (2022). Engineering of ultra-high performance self-compacting mortar with recycled steel fibres extracted from waste tires. Archives of Civil and Mechanical Engineering, 22: 175. https://doi.org/10.1007/s43452-022-00496-4
[43] Roshan, N., Ghalehnovi, M. (2023). The effect of recycled-tire steel fiber and engineered steel fiber on rebar corrosion and shear behavior of corroded RC beam. Case Studies in Construction Materials, 19: e02251. https://doi.org/10.1016/j.cscm.2023.e02251
[44] Prasad, C.V.S.R., Goud, K.C. (2024). Investigations on the practical use of recycled plastic in concrete. Educational Administration: Theory and Practice, 30(5): 7850-786. https://doi.org/10.53555/kuey.v30i5.4249
[45] Mohapatra, A.K., Pradhan, B. (2025). Evaluation of extent of corrosion degradation and deterioration mechanism of hybrid alkali-activated mortar subjected to sulfuric acid and hydrochloric acid solutions. Construction and Building Materials, 489: 140506. https://doi.org/10.1016/j.conbuildmat.2025.140506
[46] Wang, J., Du, B., Shen, M., Li, Y., Yuan, S. (2025). Damage constitutive model and mechanical properties of a concrete limestone composite after acid corrosion. Scientific Reports, 15: 1868. https://doi.org/10.1038/s41598-024-83364-w
[47] Meddah, M.S., Abdel-Gawwad, H., Al Owaisi, M. (2024). The role of low-quality calcined clay in enhancing the performance of cement mortar exposed to normal and aggressive media. Scientific Reports, 14: 23855. https://doi.org/10.1038/s41598-024-74885-5
[48] Yang, H., Che, Y., Leng, F. (2018). Calcium leaching behavior of cementitious materials in hydrochloric acid solution. Scientific Reports, 8: 8806. https://doi.org/10.1038/s41598-018-27255-x
[49] Fernandes, M., Neves, R. (2024). Assessment of fiber corrosion influence in the flexural performance of steel fiber-reinforced concrete. Applied Sciences, 14(13): 5611. https://doi.org/10.3390/app14135611
[50] Liu, H., Yang, L., Kang, K., et al. (2024). Mechanical properties and corrosion mechanism of steel fiber reinforced concrete (SFRC) subjected to stray current. Journal of Building Engineering, 96: 110519. https://doi.org/10.1016/j.jobe.2024.110519
[51] Kroviakov, S., Kryzhanovskyi, V., Hedulian, D. (2025). Comparison of the corrosion resistance of fiber-reinforced concrete with steel and polypropylene fibers in an acidic environment. Construction Materials, 5(1): 6. https://doi.org/10.3390/constrmater5010006
[52] Su, P., Li, M., Dai, Q., Wang, J. (2023). Mechanical and durability performance of concrete with recycled tire steel fibers. Construction and Building Materials, 394: 132287. https://doi.org/10.1016/j.conbuildmat.2023.132287
[53] Wang, Y., Chen, J. (2023). The mechanical properties and failure mechanisms of steel-fiber- and nano-silica-modified crumb rubber concrete subjected to elevated temperatures. Sustainability, 15(23): 16340. https://doi.org/10.3390/su152316340
[54] Flores Medina, D., Carolina Hernández Martínez, M., Flores Medina, N., Hernández-Olivares, F. (2023). Durability of rubberized concrete with recycled steel fibers from tyre recycling in aggressive environments. Construction and Building Materials, 400: 132619. https://doi.org/10.1016/j.conbuildmat.2023.132619
[55] Simon, A., Mobasher, B., Neithalath, N. (2024). Post-consumer carpet fibers in concrete: Fiber behavior in alkaline environments and concrete durability. Materials, 17(5): 977. https://doi.org/10.3390/ma17050977
[56] Janfeshan Araghi, H., Nikbin, I.M., Rahimi Reskati, S., Rahmani, E., Allahyari, H. (2015). An experimental investigation on the erosion resistance of concrete containing various PET particles percentages against sulfuric acid attack. Construction and Building Materials, 77: 461-471. https://doi.org/10.1016/j.conbuildmat.2014.12.037
[57] Aslani, F., Hou, L., Nejadi, S., Sun, J., Abbasi, S. (2019). Experimental analysis of fiber-reinforced recycled aggregate self-compacting concrete using waste recycled concrete aggregates, polypropylene, and steel fibers. Structural Concrete, 20(5): 1670-1683. https://doi.org/10.1002/suco.201800336
[58] Hichem, M., Kada, A., Karim, B., Azzaz, M., Mohammed, E., Leklou, N. (2024). Performance of self-compacting concrete containing recycled aggregates and recycled steel fibers. Journal of Engineering Research and Applications, 68: 51-66. https://doi.org/10.4028/p-gama0s
[59] Yu, J., Wu, Q., Zhao, D., Jiao, Y. (2025). Influence of recycled tire steel fiber content on the mechanical properties and fracture characteristics of ultra-high-performance concrete. Materials, 18(14): 3300. https://doi.org/10.3390/ma18143300
[60] Dani, M.L., Kherraf, L., Boughamsa, W., Kherraf, S., Rezaiguia, N. (2026). Experimental study on tie wire fibre and ceramic wastes in sand concrete. Annales de Chimie - Science des Matériaux, 50(2): 115-129. https://doi.org/10.18280/acsm.500202
[61] Marcos-Meson, V., Fischer, G., Edvardsen, C., Skovhus, T.L., Michel, A. (2019). Durability of steel fibre reinforced concrete (SFRC) exposed to acid attack: A literature review. Construction and Building Materials, 200: 490-501. https://doi.org/10.1016/j.conbuildmat.2018.12.051
[62] Zia, A., Pu, Z., Holly, I., Umar, T., Tariq, M.A.U.R., Sufian, M. (2022). A comprehensive review of incorporating steel fibers of waste tires in cement composites and its applications. Materials, 15(21): 7420. https://doi.org/10.3390/ma15217420
[63] Chen, Y., Waheed, M.S., Iqbal, S., Rizwan, M., Room, S. (2024). Durability properties of macro-polypropylene fiber reinforced self-compacting concrete. Materials, 17(2): 284. https://doi.org/10.3390/ma17020284
[64] Marrok, S., Belachia, M., Kherraf, L., Salhi, M., Khaldi, N. (2024). Investigating the impact of stainless steel shavings fibers 316L on enhancing the properties of high-flow sand concrete in the long-term. Annales de Chimie - Science des Matériaux, 48(4): 529-537. https://doi.org/10.18280/acsm.480410

[65] Lee, K.M., Bae, S.H., Park, J.I., Kwon, S.O. (2015). Mass change prediction model of concrete subjected to sulfate attack. Mathematical Problems in Engineering, 2015(1): 298918. https://doi.org/10.1155/2015/298918
[66] Ziane, S., Khelifa, M.R., Mezhoud, S., Beroual, A., Medaoud, S. (2021). Experimental study on the durability characteristics of several vegetable fiber reinforced concretes exposed to sodium sulfate. Civil and Environmental Engineering Reports, 31(1): 1-28. https://doi.org/10.2478/ceer-2021-0001
[67] Qin, S., Chen, C., Zhang, M. (2024). Modeling of concrete deterioration under external sulfate attack and drying–wetting cycles: A review. Materials, 17(13): 3334. https://doi.org/10.3390/ma17133334
[68] Liu, Y., Wang, L., Cao, K., Sun, L. (2021). Review on the durability of polypropylene fibre-reinforced concrete. Advances in Civil Engineering, 2021(1): 6652077. https://doi.org/10.1155/2021/6652077
[69] Lu, S., Liu, J., Tian, Z., et al. (2025). Deterioration mechanisms and strength prediction of hybrid fiber-reinforced concrete under coupled sulfate attack and dry-wet cycles. Construction and Building Materials, 493: 143243. https://doi.org/10.1016/j.conbuildmat.2025.143243
[70] Guo, J., Wang, K., Qi, C. (2021). Determining the mineral admixture and fiber on mechanics and fracture properties of concrete under sulfate attack. Journal of Marine Science and Engineering, 9(3): 251. https://doi.org/10.3390/jmse9030251
[71] Biscaro, C., Martínez, A., Pérez, A., Xotta, G., López, C.M., Carol, I. (2024). 'Onion-peel' cracking and spalling in coupled meso-mechanical analysis of external sulfate attack in concrete using zero-thickness interface elements. Construction and Building Materials, 455: 139011. https://doi.org/10.1016/j.conbuildmat.2024.139011
[72] Belferrag, A., Meziani, N., Kriker, A. (2025). Enhancement of sulfate resistance in dune sand mortars through polypropylene fiber incorporation. Periodica Polytechnica Civil Engineering, 69(4): 1345-1353. https://doi.org/10.3311/ppci.42005
[73] Qin, Y., Liu, J., Xu, C., Dang, F., Zhou, H., Shi, L. (2023). Experimental study and evaluation of bonding properties between fiber and cement matrix under sulfate attack. Journal of Building Engineering, 76: 107306. https://doi.org/10.1016/j.jobe.2023.107306
[74] Ran, T., Pang, J., Yu, J. (2023). Performance of rubber concrete containing polypropylene and basalt fibers under coupled sulfate attack and freeze–thaw conditions: An experimental evaluation. Polymers, 15(9): 2066. https://doi.org/10.3390/polym15092066
[75] Tang, Q., Chai, S., Hou, D., et al. (2024). Unraveling concrete's interfacial transition zone vulnerability under erosive environments: A molecular dynamics study. Journal of Building Engineering, 94: 110046. https://doi.org/10.1016/j.jobe.2024.110046
[76] Hilbig, H., Gutberlet, T., Beddoe, R.E. (2024). Acid attack on hydrated cement: Effect of organic acids on the degradation process. Materials and Structures, 57: 83. https://doi.org/10.1617/s11527-024-02360-8
[77] Ecemiş, A.S., Yildizel, S.A., Beskopylny, A.N., et al. (2025). Sustainable concrete with waste tire rubber and recycled steel fibers: Experimental insights and hybrid PINN–CatBoost prediction. Polymers, 17(21): 2910. https://doi.org/10.3390/polym17212910
[78] Kantarcı, F. (2022). Influence of fiber characteristics on sulfate resistance of ambient-cured geopolymer concrete. Structural Concrete, 23(2): 775-790. https://doi.org/10.1002/suco.202100540